π^0 decay process of $^{12}_{\Lambda}$C and $^{11}_{\Lambda}$B hypernuclei

A. Sakaguchi,* W. Brückner, S. Paul, R. Schüssler, and B. Povh
Max-Planck-Institut für Kernphysik, Heidelberg D-6900, Federal Republic of Germany

H. Döbbeling
Physikalisches Institut der Universität Heidelberg, Heidelberg D-6900, Federal Republic of Germany

M. Aoki, H. Tamura,† and T. Yamazaki
Institute for Nuclear Study, University of Tokyo, Tanashi, Tokyo 188, Japan

R. S. Hayano, T. Ishikawa, M. Iwasaki, T. Motoki, H. Outa, E. Takada
Department of Physics, University of Tokyo, Tokyo 113, Japan

K. H. Tanaka
National Laboratory for High Energy Physics (KEK), Tsukuba, Ibaraki 305, Japan
(Received 30 August 1990)

We investigated π^0 decay branching ratios Γ_{π^0}/Γ in the weak decay of the $^{12}_{\Lambda}$C and $^{11}_{\Lambda}$B hypernuclei using the (stopped K^-,π^-) reaction. The branching ratios were estimated to be $0.174\pm0.057(\text{stat})\pm0.008(\text{syst})$ and $0.140\pm0.039(\text{stat})\pm0.025(\text{syst})$ for the $^{12}_{\Lambda}$C and $^{11}_{\Lambda}$B hypernuclei, respectively. The branching ratios are compared with theoretical calculations and related experimental values. Importance of distortion of pion wave function was found.

I. INTRODUCTION

As is well known, a free Λ particle mainly decays into a pair consisting of a nucleon and a pion ($\Lambda\rightarrow p+\pi^-, n+\pi^0$). A bound Λ particle in a nucleus or a Λ particle in a Λ hypernucleus also decays into a pair consisting of a nucleon and a pion. This decay process of the Λ hypernucleus is the mesonic decay process. The bound Λ particle can interact with a neighboring nucleon and can decay also into a nucleon ($\Lambda+N\rightarrow N+N$). The process is called the nonmesonic decay process. While the nonmesonic decay process provides a unique opportunity to study Λ-N weak interaction, the existence of internuclear cascade processes obstruct experimental studies, and theoretical understanding of the process has not been established. On the other hand, the mesonic decay process has been well formulated for the decay of Λ hypernuclei as well as the free Λ decay. The formula has been well established, especially for the mesonic decay process in very light Λ hypernuclei, and has been used to determine the ground-state spins[1] of hypernuclei. For heavier Λ hypernuclei, however, there have been few theoretical calculations which reproduce experimental observations. The mesonic decay process in the heavier Λ hypernuclei is characterized by a suppression that comes from the Pauli blocking, because, in the process, an additional nucleon is created in the nucleus and the recoil momentum of the nucleon ($p_N\approx 100$ MeV/c) is smaller than the Fermi momentum of nucleons. Recently, several theoretical improvements have been made, and these theories predict that the suppression is sensitive to the degree of occupation of inner shell-model orbits,[2] which is difficult to probe by normal nuclear reactions, and is also sensitive to the pion wave function in the final state.[3]

Experimentally, the decay process of Λ hypernuclei was studied in 1960s with emulsion and bubble-chamber experiments, where the information on the decay was limited to few Λ hypernuclei or an averaged feature over many Λ hypernuclei. This came from the difficulty in selective formation of Λ hypernuclei and in its unique identification.

After several successful counter experiments[4,5] on strangeness-exchange reactions, the first study of the decay process by a counter experiment was reported for the in-flight (K^-,π^-) reaction on ^{12}C and ^{6}Li targets by Grace *et al.*[6] In the experiment the formation of Λ hypernuclei was uniquely identified by the measurement of the π^- momentum from the in-flight (K^-,π^-) reaction. They extracted the total decay widths for the $^{12}_{\Lambda}$C, $^{11}_{\Lambda}$B, and $^{5}_{\Lambda}$He hypernuclei.

Recently, we investigated the π^0 decay process of the $^{12}_{\Lambda}$C and $^{11}_{\Lambda}$B hypernuclei by a counter experiment utilizing the K^- absorption reaction at rest. This is the first direct measurement of the π^0 decay branching ratios[7,8] of the Λ hypernuclei. In this paper we describe the experimental setup in Sec. II and the procedure to extract the π^0 decay branching ratios in Sec. III. Results of the comparison with a theoretical calculation will be made in Sec. IV and discussions in Sec. V.

II. EXPERIMENTAL SETUP

We investigated the π^0 decay of the $^{12}_{\Lambda}$C and $^{11}_{\Lambda}$B hypernuclei by a π^0 coincidence measurement in the (stopped

K^-,π^-) reaction. The experimental setup was an improved one over the previous experment.[9] The measurement was made at the low-energy kaon beam line[10] (K3 beam line) of the 12-GeV proton synchrotron (PS) at the National Laboratory for High Energy Physics (KEK). Figure 1 shows the configuration of beam-line elements of the K3 beam line. Kaons of 650 MeV/c momentum were transported to the reaction target (RT) point. For the measurement of the K^- absorption reaction at rest, two graphite degraders (GD1 and GD2), three lucite Čerenkov counters (LC1–LC3), two beam defining counters of plastic scintillator (B2 and B3), and two multiwire proportional chambers (MWPC's) with 1-mm spacing x-y-u planes (BC1 and BC2) were installed in the beam line. The combination of the kaon momentum of 650 MeV/c and the graphite degrader was optimized for the stopping kaon yield in the reaction target. The kaon yield was determined by the competition of an exponential increase of kaon yield, a decrease of kaon stopping density, and a decrease of kaon flux by scattering and reaction in a graphite degrader with increase of kaon momentum. The lucite Čerenkov counters were used as pion vetos. The kaon intensity at the reaction target point was about 1700K^-/burst (0.5-sec burst in 2.5 sec) at a primary 12-GeV proton beam intensity of 1.0×10^{12} protons/burst.

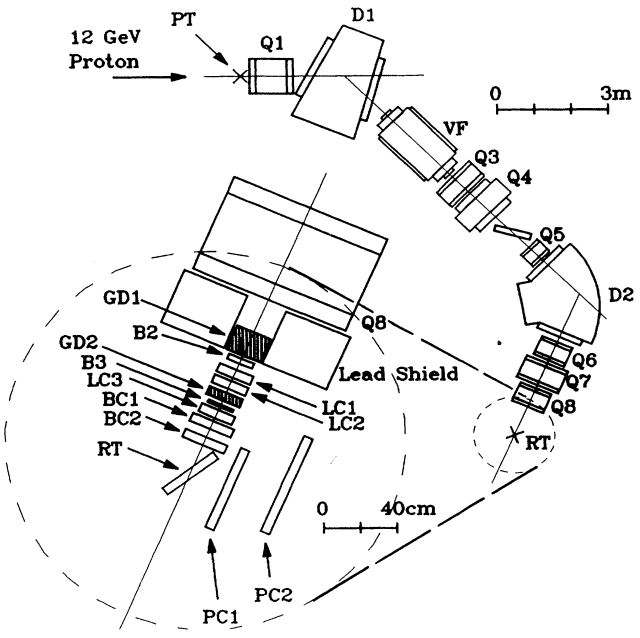

FIG. 1. Configuration of the low-momentum kaon beam line (K3) at KEK 12-GeV PS. The beam line consists of a production target (PT), elements for beam transport ($D1$, $D2$, and $Q1$–$Q8$) and a velocity filter (VF, 2-m-long dc mass separator). The distance from the production target to the reaction target (RT) is 15.3 m. To stop kaons in the reaction target, graphite degraders (GD1 and GD2) were installed in the beam line. In the beam line, three lucite Cerenkov counters (LC1–LC3), two defining scintillation counters (B2 and B3), and two tracking MWPC's were also installed.

A plastic-scintillator stack was used as the reaction target. The scintillator stack consisted of 16 layers of plastic scintillation counters of 3 mm in thickness. The size of the target was 48 mm in total thickness of 16 layers, 150 mm in height, and 350 mm in width. the target was located at the reaction target point, tilted by 60° (see Fig. 1), so that the target was thick along the kaon beam trajectory and thin along the outgoing pion trajectory. The number of stopping kaons in the target was estimated to be about 1100 K^-/burst at a primary proton beam intensity of 1.0×10^{12} protons/burst.

As shown in Fig. 2, the identification and momentum determination of outgoing pions were made with a large-acceptance magnetic spectrometer (SP), four tracking gas chambers (PC1, PC2, DC3, and DC4), a time-of-flight (TOF) counter, and a range counter stack (RNG). The spectrometer was a C-type magnet with rectangular poles operated with a field strength of 11.7 kG, employing vertical focusing by the oblique entry to the homogeneous field. The typical solid angle of the spectrometer was 80 msr over the momemtum range from 130 to 280 MeV/c. Two of the tracking gas chambers (PC1 and PC2) were two-dimensional cathode-readout chambers. For the other two gas chambers (DC3 and DC4), the y coordinate was measured from drift time in a 32-mm drift cell, and the x coordinate was measured by cathode readout. The typical position resolutions of the tracking gas chambers were 320 and 700 μm [full width at half maximum (FWHM)] for the cathode readout and drift chambers, respectively. The time-of-flight counter was a plastic-scintillation counter of 4 cm in thickness. The range

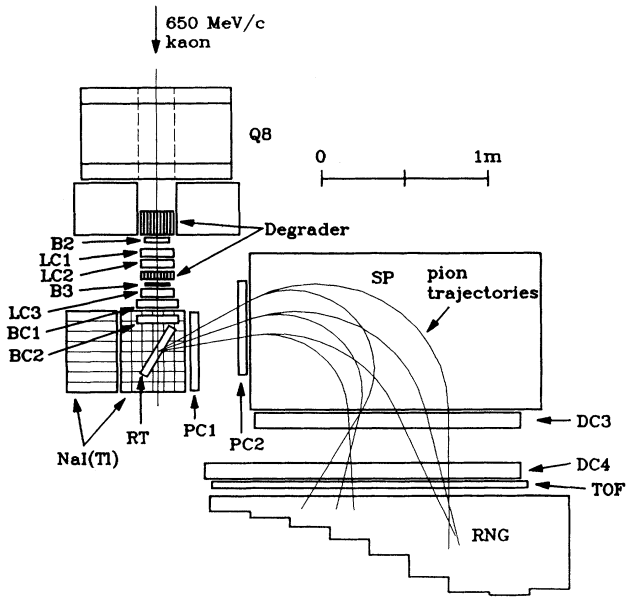

FIG. 2. Schematic view of the experimental setup. The momentum of the outgoing pions is analyzed by the magnetic spectrometer (SP) and tracking wire chambers (PC1, PC2, DC1, and DC2). The pions are discriminated from contaminant negative muons and electrons by the time-of-flight (TOF) and range (RNG) counters. The reaction target (RT) is surrounded by NaI(Tl) scintillation counters to detect decay particles.

counter stack consisted of 85 modules of plastic-scintillation counter of 2 cm in thickness. Contaminant muons, which came from in-flight decay of pions and kaons, were rejected by using the information from the range counter stack with a rejection efficiency of 95%. The pion momentum was evaluated by an integration of the equation of motion employing the result of magnetic-field mapping. The intrinsic momentum resolution of the spectrometer system was about 1.8 MeV/c (FWHM) at around 260 MeV/c.

Since the energy loss of outgoing pions in the reaction target was not negligible in determining the momentum of the pions to good precision, the reaction point in the target was determined from the kaon and pion trajectories reconstructed from hit positions at four tracking chambers (BC1, BC2, PC1, and PC2). The pion momentum measured with the spectrometer system was corrected for the energy loss of the pion calculated from the outgoing pion path in the target. The overall momentum resolution of outgoing pions was about 3.8 MeV/c (FWHM) at 236 MeV/c. The contribution from the ambiguity of reaction point determination to the momentum resolution was about 2.6 MeV/c. Another major contribution to the momentum resolution came from energy-loss straggling of outgoing pions.

To detect decay products of hypernuclei, the reaction target was surrounded by 176 modules of NaI(Tl) counters. The size of each NaI(Tl) module was 65 mm$\times$65 mm$\times$300 mm. The NaI(Tl) counters covered a solid angle of about 50% of 4π sr. In front of the NaI(Tl) counters, plastic-scintillation counters of 4 mm in thickness were placed as ΔE counters. They served also as counters to discriminate between a charged particle and neutral particle. The energy calibration of the NaI(Tl) counters was made with gamma rays from a ^{88}Y gamma-ray source and with monochromatic muons (p_μ=236 MeV/c) from the $K_{\mu 2}$ decay of a K^+ particle ($K^+ \rightarrow \mu^+ + \nu$ decay) at rest. The typical energy resolution for the 236-MeV/c muons was 14% (FWHM).

The trigger condition (TRIG) of the data acquisition was as follows:

$$\text{TRIG} = \text{B2} \times \text{B3} \times \overline{\text{LC1}} \times \overline{\text{LC2}} \times \overline{\text{LC3}} \times \text{RT1} \times \text{PC2} \times \text{TOF} ,$$

where RT1 indicated a particle hit in the first layer of the scintillator target stack. The typical trigger rate under the trigger condition was 10 events/burst. The total run time for measurement was 284 h and the total number of stopped kaons in the target was 6.17×10^8 kaons.

III. ANALYSES

Figure 3 shows a pion momentum spectrum from the (stopped K^-,π^-) reaction on a carbon target [plastic scintillator $(CH)_n$]. In the spectrum two clear peaks are observed at the pion momenta of 273.1$\pm$0.2 and 261.1$\pm$0.2 MeV/c. These peaks correspond to the formation of the well-known states in the $^{12}_{\Lambda}$C hypernucleus. The peak at 273.1 MeV/c is identified as the ground state of $^{12}_{\Lambda}$C with a (s_Λ, p_n^{-1}) shell-model configuration (Λ binding energy is 11.1 MeV), and the peak at 261.1 MeV/c is assigned to the cluster of excited states at around 11 MeV excitation energy with a (p_Λ, p_n^{-1}) configuration (Λ binding energy is 0.1 MeV). The ground state of $^{12}_{\Lambda}$C decays with the mesonic and nonmesonic weak decay modes. The 11-MeV excited states of $^{12}_{\Lambda}$C decay with proton emission to the ground state of the $^{11}_{\Lambda}$B hypernucleus,[11] which, then, decays with the mesonic and nonmesonic weak decay modes. So these peaks are related to the weak decays of the ground states in $^{12}_{\Lambda}$C and $^{11}_{\Lambda}$B hypernuclei, respectively.

To investigate the π^0 decay process of the hypernuclei, π^0 coincidence events were selected. In the π^0 identification, two gamma rays from π^0 decay were detected with the NaI(Tl) counters, and calculations of the invariant mass were made from the momenta of the gamma rays. In the detection of the gamma rays, charged particles were vetoed by the ΔE plastic scintillation counters in front of the NaI(Tl) detectors, and slow neutrons were excluded using the time of flight between the target and the NaI(Tl) detectors. Figure 4 shows a spectrum of the invariant mass in the (stopped K^-,π^-) reaction. For the invariant-mass spectrum, the π^- momentum region from 220 to 280 MeV/c was selected. The selected region corresponds to the momentum region of the quasifree Λ formation process and of the formation process of hypernuclei. The solid line in the figure indicates an expected shape of the invariant-mass spectrum estimated by a Monte Carlo simulation (the momentum of π^0 was assumed to be 100 MeV/c). The invariant-mass spectrum obtained from the experimental data was in good agreement with the simulation above 60 MeV.

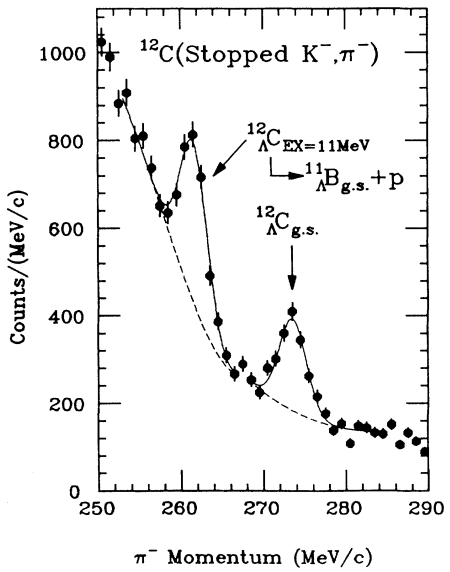

FIG. 3. Momentum spectrum of negative pions from the kaon absorption reaction at rest. Two pronounced peaks are observed at pion momenta of 273.1 and 261.1 MeV/c, which correspond to the formation of the ground and 11-MeV excited states in the $^{12}_{\Lambda}$C hypernucleus, respectively. The solid curves in the figure show the results of the peak fitting.

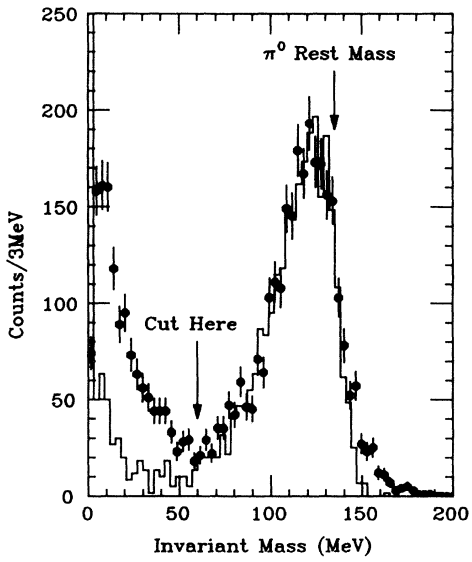

FIG. 4. Spectrum of the invariant mass of two gamma rays detected by the NaI(Tl) counters in the (stopped K^-,π^-) reaction. The π^- momentum region from 220 to 280 MeV/c was selected to see the invariant-mass spectrum of π^0 particles coming from the decay of Λ particles created in the quasifree Λ formation process and from the decay of hypernuclei. The solid line shows the result of a Monte Carlo simulation.

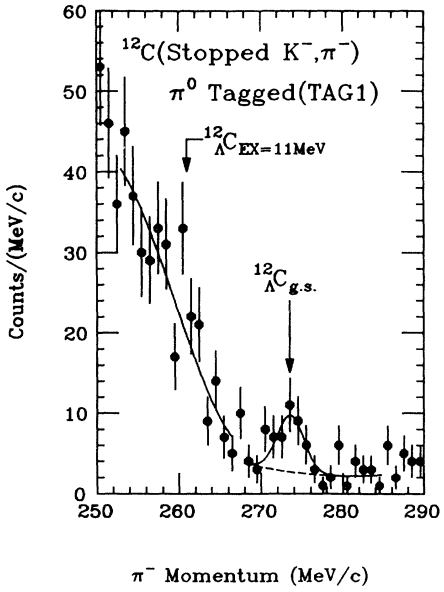

FIG. 5. Momentum spectrum of the (stopped K^-,π^-) reaction in coincidence with a π^0 particle. The solid curves shows the result of the peak fitting.

Therefore, when the calculated invariant mass was greater than 60 MeV, the event was identified to be a π^0 coincident event.

Figure 5 shows the π^- momentum spectrum for the π^0 coincidence events. The peak at 273.1 MeV/c, which corresponds to the $^{12}_{\Lambda}$C ground state, is observed in the π^0 coincident spectrum, but the peak at 261.1 MeV/c, which corresponds to the 11-MeV excited states, is less clear. From the π^0 coincidence spectrum, we estimated the π^0 decay branching ratio for the $^{12}_{\Lambda}$C decay and, at this stage, an upper limit of the branching ratio for the $^{11}_{\Lambda}$B decay. Peak counts were estimated for the 273.1- and 261.1-MeV/c peaks in Figs. 3 and 5 by a peak fitting. In the peak fitting, a Gaussian function was employed as the peak shape, and common parameters of the peak width and position were used for both spectra. As a shape of the underlying background, a polynomial function was used. The results of the peak fitting are shown with solid curves in Figs. 3 and 5.

To determine the π^0 decay branching ratios, an estimation of the π^0 detection efficiency of the NaI(Tl) detector system was necessary. Estimation of the π^0 detection efficiency was made by a Monte Carlo simulation program using the computer code EGS4. In the estimation an isotropic distribution of the outgoing π^0 was assumed, and a realistic distribution of the reaction points in the target was used. The conversion process of a gamma ray to an electron-positron pair in the target was also considered. The estimated detection efficiency is about 20%, as shown in Fig. 6 (solid curve).

The estimated π^0 detection efficiency was checked by experimental data of the $K_{\pi 2}$ decay ($K^+ \rightarrow \pi^+ + \pi^0$ decay) at rest ($p_{\pi^0}=205$ MeV/c), since we accumulated data on the K^+ decay at rest under the same experimental condition only by changing the polarity of the beamline magnets. A small correction was needed for contributions of π^0 particles from decay modes other than $K_{\pi 2}$. The π^0 detection efficiency obtained from the $K_{\pi 2}$ decay data is shown in the Fig. 6 (solid circle). The experimentally extracted π^0 detection efficiency is in good agree-

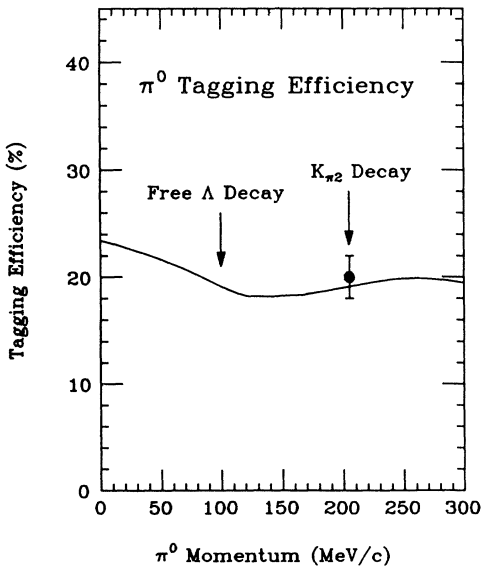

FIG. 6. π^0 detection efficiency in the invariant-mass-cut analysis. The efficiency was estimated with a Monte Carlo simulation (solid curve). The π^0 detection efficiency determined experimentally from the data of $K_{\pi 2}$ decay of K^+ particles is shown by a solid circle.

ment with the calculated efficiency.

The π^0 decay branching ratios of the ground states in the $^{12}_{\Lambda}$C and $^{11}_{\Lambda}$B hypernuclei were calculated from the peak counts and the estimated detection efficiency. Though the momenta of π^0 particles from the hypernuclear decays may have a distribution of about 10 MeV/c in width, the momenta of π^0 particles were approximated to 123.7 and 114.3 MeV/c for the $^{12}_{\Lambda}$C and $^{11}_{\Lambda}$B decay, respectively. The error of the detection efficiency from the approximation was estimated to be less than 4%. The results of the calculation of the branching ratios are listed in Table I (labeled "TAG1 POLY"). In the table the first errors of the branching ratios are statistical ones. The second errors are systematic ones coming from the π^0 detection efficiency calculation and the approximation of the π^0 momenta. The systematic error in the detection efficiency calculation was estimated from the stability of the efficiency against the change of parameters used in the Monte Carlo simulation, e.g., energy lower limits of particles and tracking step sizes. The statistical error in the Monte Carlo simulation was a minor contribution.

In the above analysis, unfortunately, a finite branching ratio was not extracted for the $^{11}_{\Lambda}$B decay. The reason for this came partly from the poor statistics of the π^0 coincidence spectrum. To get a better statistics, we made another analysis, in which a π^0 particle was identified by a detection of a gamma ray with energy larger than 50 MeV. In the (stopped K^-,π^-) reaction in the π^- momentum region of interest, the decay of π^0 particles is the primary source of energetic gamma rays, and there is no significant background of energetic gamma rays. A merit of the analysis is that it achieves a detection efficiency about 3 times larger than that of the π^0 decay analysis by the invariant-mass calculation. A possible background in the analysis may be a misidentification of a neutron as a gamma ray. To avoid the misidentification, a size larger than one NaI(Tl) module (6.5 cm$\times$6.5 cm) was required as a transverse size of the electromagnetic cascade by a gamma ray.

Figure 7 shows the π^- momentum spectrum in coincidence with gamma rays with energies larger than 50 MeV. In the figure we see the formation peak of the $^{12}_{\Lambda}$C and $^{11}_{\Lambda}$B hypernuclei. Results of a peak fitting of the 273.1- and 261.1-MeV/c peaks are shown in Fig. 7 with solid curves. The detection efficiency of gamma rays with energies larger than 50 MeV from a π^0 decay was estimated by the Monte Carlo simulation and is shown in Fig. 8. The π^0 decay branching ratios obtained in this analysis are listed in Table I (labeled "TAG2 POLY"). The estimated π^0 branching ratio of the $^{12}_{\Lambda}$C decay can be compared with the result of the previous analysis. The two branching ratios of the $^{12}_{\Lambda}$C decay ("TAG1 POLY" and "TAG2 POLY") agree with each other within the error.

In the above discussion, we estimated systematic errors of the branching ratios only from the detection efficiency

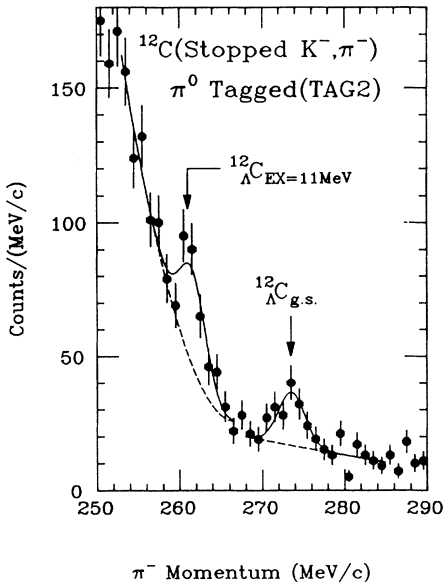

FIG. 7. π^- momentum spectrum in coincidence with a gamma ray with an energy larger than 50 MeV. The solid curves in the figure are the results of the peak fitting.

TABLE I. Branching ratios of π^0 decay for the $^{12}_{\Lambda}$C and $^{11}_{\Lambda}$B hypernuclei. Two types of π^0 event selections or taggings were made (TAG1 and TAG2), and two types of fitting functions were used (POLY and SQRT). The first error corresponds to a statistical error, and the second one corresponds to a systematical one.

Tagging type and fitting function type	π^0 decay branching ratios Γ_{π^0}/Γ $^{12}_{\Lambda}$C	$^{11}_{\Lambda}$B
TAG1 POLY	0.174±0.057±0.008	<0.240[a]
TAG2 POLY	0.156±0.041±0.002	0.165±0.044±0.002
TAG2 SQRT		0.115±0.034±0.002

[a]90% confidence limit.

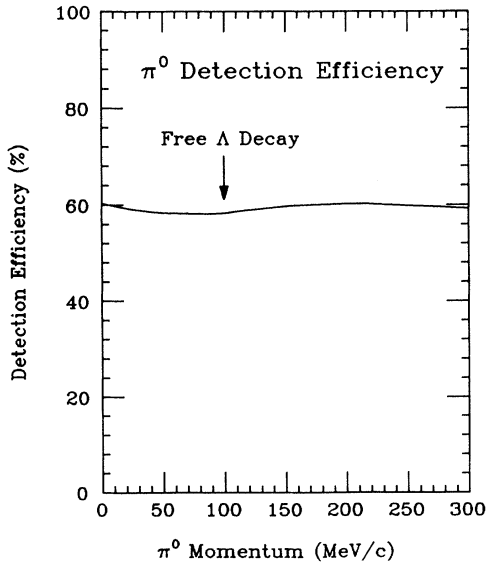

FIG. 8. Detection efficiency of a gamma ray with an energy larger than 50 MeV from a π^0 particle decay.

calculation. There may be another systematic error from the peak fitting, especially for the $^{11}_{\Lambda}$B decay branching ratio. Since the π^- momentum of the peak of the 11-MeV excited state in the $^{12}_{\Lambda}$C hypernucleus is near the threshold momentum of the quasifree Λ formation process ($K^-+n\rightarrow\pi^-+\Lambda$ process), the polynomial background shape used in the peak fitting may be inadequate. So we made another peak fitting with a different background shape. In the peak fitting, the threshold nature is simulated with a square-root function, and we defined a background shape as follows:

$$A_1 f(p_0-p)+A_2(p_0-p)+A_3 ,$$

$$f(p_0-p)=\frac{1}{\sqrt{2\pi}\sigma}\int_{-\infty}^{+\infty} g(p_0-p+q)\times\exp\left[-\frac{(q-p)^2}{2\sigma^2}\right]dq ,$$

$$g(p_0-p)=\begin{cases}\sqrt{p_0-p} & (p<p_0)\\ 0 & (p\geq p_0),\end{cases}$$

where p_0 is the threshold momentum of the quasifree process ($p_0=260.9$ MeV/c). σ is a width parameter of the Gaussian function used as the peak shape which characterized the momentum resolution of the magnetic spectrometer system. Since the square-root function changes rapidly near the threshold momentum p_0, the smearing by momentum resolution is needed (integration in the above equations). In the above background shape, we still include a background, which shape is linear with momentum, to simulate contributions from in-flight kaon decays and in-flight reactions. The result of the peak fitting with the new background shape is shown in Fig. 9 with solid curves. An estimated π^0 branching ratio of the $^{11}_{\Lambda}$B weak decay is listed in the Table I (labeled "TAG2 SQRT").

There is an obvious difference between the π^0 decay branching ratios of the $^{11}_{\Lambda}$B hypernucleus estimated by the peak fitting procedures with different background shapes. We consider that the branching ratios for the $^{11}_{\Lambda}$B decay estimated from the above analyses are an upper and a lower bounds of the branching ratio (the adequacy of this assumption will be mentioned in Sec. V), respectively, and take the difference of the branching ratios to be an additional systematic error which comes from the ambiguity in the peak fitting procedure. So we obtained the following averaged π^0 decay branching ratio for the $^{11}_{\Lambda}$B decay:

$$\Gamma_{\pi^0}/\Gamma=0.140\pm0.039(\text{stat})\pm0.025(\text{syst}) .$$

For the $^{12}_{\Lambda}$C decay, since the shape of the background in the π^- momentum spectrum is expected to change smoothly with pion momentum, the systematic error coming from the ambiguity of the peak fitting is much less than that in the analysis of the $^{11}_{\Lambda}$B decay.

IV. RESULTS

In the following we will compare the experimental result obtained in the present experiment with theoretical predictions. To compare the measured π^0 decay branching ratios Γ_{π^0}/Γ with theoretical π^0 partial decay widths Γ_{π^0}, we need the total decay widths Γ. We adapted the total width values obtained from a lifetime measurement by Grace *et al.*,[4] who reported $\Gamma=(1.25\pm0.18)\Gamma_{\Lambda}$ for $^{12}_{\Lambda}$C and $\Gamma=(1.37\pm0.16)\Gamma_{\Lambda}$ for $^{11}_{\Lambda}$B hypernuclei. We then obtained the π^0 partial decay widths for $^{12}_{\Lambda}$C and $^{11}_{\Lambda}$B hypernuclei, and the results are listed in Table II. The π^0

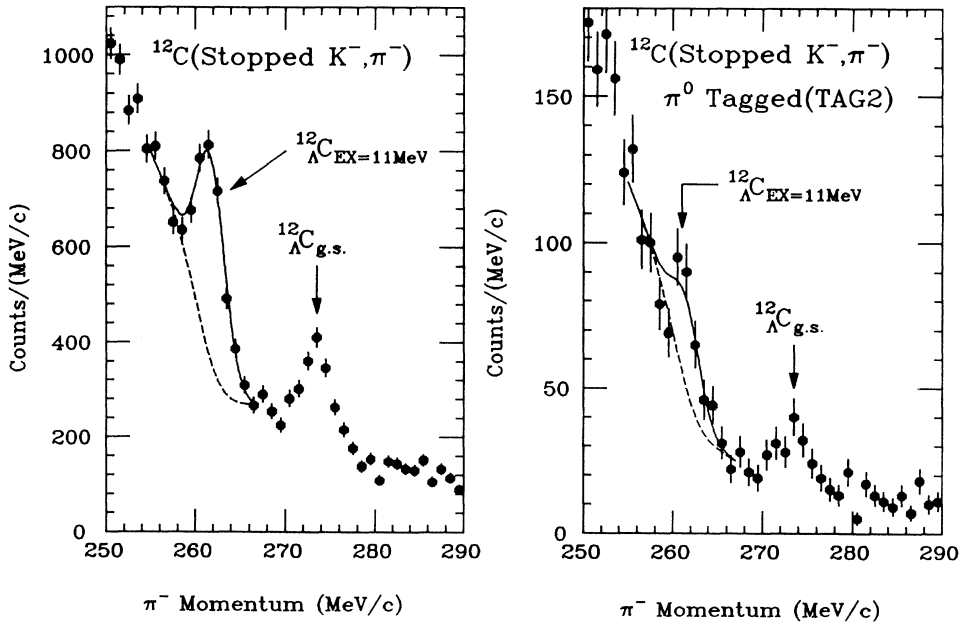

FIG. 9. Result of peak fitting with a square-root-shaped background function.

TABLE II. Experimental and theoretical mesonic decay widths.

Hypernucleus and decay mode		Experiments: Present	Barnes and Szymanski (Ref. 6)	Montwill *et al.*[b]	Theory (Ref. 3)[a]: Free	MSU	WHIS
$^{12}_{\Lambda}$C	π^0	$(0.217\pm0.073\pm0.011)\Gamma_\Lambda$			$0.078\Gamma_\Lambda$	$0.169\Gamma_\Lambda$	$0.126\Gamma_\Lambda$
	π^-		$(0.051\pm0.045)\Gamma_\Lambda$		$0.058\Gamma_\Lambda$	$0.134\Gamma_\Lambda$	$0.107\Gamma_\Lambda$
$^{11}_{\Lambda}$B	π^0	$(0.192\pm0.056\pm0.034)\Gamma_\Lambda$			$0.063\Gamma_\Lambda$	$0.140\Gamma_\Lambda$	$0.104\Gamma_\Lambda$
	π^-			$(0.218\pm0.046)\Gamma_\Lambda$	$0.134\Gamma_\Lambda$	$0.294\Gamma_\Lambda$	$0.223\Gamma_\Lambda$

[a]The lower spin state of the spin doublet was assumed to be the ground state.
[b]Estimated from $Q^- = \Gamma_{nm}/\Gamma_{\pi^-}$ in Ref. 12.

decay widths estimated from our data are about 60% and 50% of the π^0 decay width of the free Λ particle for the $^{12}_{\Lambda}$C and $^{11}_{\Lambda}$B hypernuclei, respectively. If we take into account the enhancement factor $N+1$ from antisymmetrization,[1] where N is the neutron number of the hypernuclei and is 3 for the $p_{3/2}$ shell-model orbit, the decay widths correspond to a suppression to about 15% of the π^0 decay width of the free Λ particle.

Recently, a realistic shell-model calculation for the mesonic decay widths of the hypernuclei with mass numbers from $a=7$ to 15 was made by Motoba, Itonaga, and Bandō.[3] In the calculation they used three different types of pion wave function in the final state, and they reported a large dependence of the calculated mesonic decay widths on the pion wave functions to be used. Interpretation is as follows. The pion-nucleus interaction changes the local momentum of pions and brings a component of the wave function with higher momentum transfer than that without the pion-nucleus interaction. The component with the larger momentum transfer is relatively free from the Pauli blocking of the nucleon and contributes to the decay process. So the degree of the distortion of the pion wave function affects the mesonic decay width. The predictions of the theoretical calculation of Motoba, Itonaga, and Bandō are also listed in Table II for comparison. Since the lambda particle has the spin, it forms a low-lying spin doublet with a core nuclear spin, and the theoretical decay widths depend on the ground-state spin. In the following we will assume that the lower spin state of the spin doublet is the ground state.

From Table II it is seen that the π^0 decay widths are near the theoretical prediction referred as MSU (Michigan State University), for which the calculation is made with the optical potential parameters of the MSU group in the pion wave-function calculation. The MSU optical potential has a strong imaginary part and a strong distortion. Furthermore, the theoretical prediction with the free pion wave function has the largest deviation from the experimental width. The result seems to show that the distortion of the pion wave function is considerably large in the nucleus and enhances the mesonic decay width.

Motoba, Itonaga, and Bandō also pointed out[3] that the ratios of the π^0 and π^- decay widths, $\Gamma_{\pi^0}/\Gamma_{\pi^-}$, and the ratios of the mesonic decay widths of different hypernuclei were relatively stable under the change of the pion wave functions. Experimental ratios of the mesonic decay widths are listed in Table III with the theoretical model prediction. In the table the experimental ratio $\Gamma_{\pi^0}(^{12}_{\Lambda}\mathrm{C})/\Gamma_{\pi^0}(^{11}_{\Lambda}\mathrm{B})$ obtained from the present data is in good agreement with the theoretical prediction.

Next, we will see the $\Gamma_{\pi^-}/\Gamma_{\pi^0}$ ratio. The π^- decay width for the $^{12}_{\Lambda}$C was estimated by Barnes and Szymanski[4] and is listed in Table II. Another measurement on the π^- decay process was made in the emulsion counter experiment[12] for the $^{11}_{\Lambda}$B hypernucleus. The ratio $Q^- = \Gamma_{NM}/\Gamma_{\pi^-} = 4.8\pm1.1$ was reported by the experiment, and so we can estimate the π^- decay width Γ_{π^-} by the following assumptions and the total decay width Γ from Ref. 6:

$$\Gamma_{\pi^-}/\Gamma_{\pi^0} = 2 ,$$

$$\Gamma_{\pi^-} + \Gamma_{\pi^0} + \Gamma_{NM} = \Gamma ,$$

where Γ_{NM} is the nonmesonic decay widths. Theoretically, the first equation is a result of the $\Delta I = \frac{1}{2}$ enhancement in the strange particle decay and the similarity of the nuclear structures in daughter nuclei. The second equation is a definition of the nonmesonic decay width. The result of the estimation is listed in Table II. From these π^- decay widths and our π^0 decay widths, the experimental $\Gamma_{\pi^-}/\Gamma_{\pi^0}$ ratios in the $^{12}_{\Lambda}$C and $^{11}_{\Lambda}$B decays were estimated and are listed in Table III. For the $\Gamma_{\pi^-}/\Gamma_{\pi^0}$ ratio in the $^{12}_{\Lambda}$C decay, the experimental ratio is much lower than the theoretical prediction and has a large error which mainly comes from the error in the experimental π^- decay width. A possible explanation of the smaller experimental $\Gamma_{\pi^-}/\Gamma_{\pi^0}$ ratio is that the experimental π^- decay width is too small. When we estimate the ratio $\Gamma_{\pi^-}(^{12}_{\Lambda}\mathrm{C})/\Gamma_{\pi^-}(^{11}_{\Lambda}\mathrm{B})$ from the experimental data, we obtain

$$\Gamma_{\pi^-}(^{12}_{\Lambda}\mathrm{C})/\Gamma_{\pi^-}(^{11}_{\Lambda}\mathrm{B}) = 0.24^{+0.23}_{-0.20} ,$$

TABLE III. Experimental ratios of the mesonic decay widths and theoretical predictions.

Ratio		Experiment	Theory (Ref. 3)
$\Gamma_{\pi^0}(^{12}_{\Lambda}\mathrm{C})/\Gamma_{\pi^0}(^{11}_{\Lambda}\mathrm{B})$		$1.13^{+0.63}_{-0.43}\pm0.21$	1.22 ± 0.02
$\Gamma_{\pi^-}/\Gamma_{\pi^0}$	$^{12}_{\Lambda}$C	$0.24^{+0.26}_{-0.20}\pm0.01$	0.79 ± 0.05
	$^{11}_{\Lambda}$B	$1.13^{+0.49}_{-0.30}\pm0.22$	2.13 ± 0.01

while the theory predicts

$$\Gamma_{\pi^-}({}^{12}_{\Lambda}\mathrm{C})/\Gamma_{\pi^-}({}^{11}_{\Lambda}\mathrm{B})=0.46\pm0.02 \ .$$

This result is consistent with the explanation that the experimental π^- decay width of the ${}^{12}_{\Lambda}$C is too small.

For the $\Gamma_{\pi^-}/\Gamma_{\pi^0}$ ratio in the ${}^{11}_{\Lambda}$B decay, the experimental ratio is about a half of the theoretical value. The theoretical $\Gamma_{\pi^-}/\Gamma_{\pi^0}$ ratio in the ${}^{11}_{\Lambda}$B decay is considered to be quite stable, because the ratio is essentially the ratio of squared Clebsch-Gordan coefficients of the isospin from the $\Delta I=\frac{1}{2}$ rule. The deviation of the experimental $\Gamma_{\pi^-}/\Gamma_{\pi^0}$ ratio from the theoretical one means an inconsistency between the experimental π^0 and π^- decay widths. So for further systematic study of the mesonic decay process in $A=10$–20 hypernuclei, we need more data on the π^- decay process as well as more π^0 decay data.

V. DISCUSSION

Although the experimental π^0 decay widths are close to the theoretical decay widths calculated with the MSU pion optical potential, the experimental widths are still larger than the theoretical widths. The nuclear wave functions of Cohen and Kurath which are used in the theoretical calculation take into account residual interactions between p-shell particles and holes, but assume a fully occupied s-shell orbit. Possible s-shell vacancies in realistic nuclear wave functions may account for the larger experimental decay widths. An enhancement factor of 1.3–1.4 is large enough to account for the larger widths. Theoretically, the enhancement factor of the mesonic decay coming from the short-range correlation was estimated to be 1.6 for the ${}^{13}_{\Lambda}$C hypernucleus.[2] Since the enhancement is expected to be significant for the hypernuclei with shell-closed core nuclei, the enhancement factor for the ${}^{12}_{\Lambda}$C and ${}^{11}_{\Lambda}$B hypernuclei is expected to be less than 1.6.

In the estimation of the π^0 decay branching ratio of the ${}^{11}_{\Lambda}$B hypernucleus, the ambiguity of the background shape causes the largest systematic error. Though the square-root background shape seems to be physically more reasonable than the background shape of the polynomial function, because the square-root shape reflects the phase-space factor near the threshold of the quasifree process, it is too simple in two points. The first point is that the threshold which we have mentioned is the threshold of the $K^-+{}^{12}\mathrm{C}\rightarrow\pi^-+\Lambda+{}^{11}\mathrm{C}_{\mathrm{g.s.}}$ reaction in which the ^{11}C nucleus stays in the ground state. There are other reactions in which the ^{11}C nucleus stays in excited states and continuum states, i.e., the $K^-+{}^{12}\mathrm{C}\rightarrow\pi^-+\Lambda+{}^{11}\mathrm{C}^*$ reaction. These reactions have lower threshold momenta than that in the $K^-+{}^{12}\mathrm{C}\rightarrow\pi^-+\Lambda+{}^{11}\mathrm{C}_{\mathrm{g.s.}}$ reaction. So a sum of many square-root functions should be used instead of the single square-root function as the background shape. The sum of the square-root functions with the smearing of momentum resolution is not so steep around the threshold energy compared with the single square-root function and is near the polynomial function. The second point is that bound states with ${}^{11}\mathrm{C}^*+\Lambda(0s)$ configuration and many broad resonance states may exist at around the threshold. By taking into account the finite momentum resolution, contributions of these states in the π^- momentum spectrum make the spectrum shape smoother at around the threshold momentum.

On the other hand, the background shape of the polynomial function does not take into account the threshold nature explicitly. So the polynomial function background shape may be too smooth. From the above considerations, a realistic background shape seems to exist between the single square-root function and the polynomial function background shapes. This is the reason for assuming that the branching ratios estimated by the two-peak fitting procedures are the upper and lower bounds of the branching ratio in the Sec. III.

In counter experiments for the study of the decay processes of hypernuclei, the detection of decay π^0 particles is relatively easy compared with a charged-particle detection. This comes partly from a longer stopping range of photons from the π^0 decay and partly from the use of a thicker target in the counter experiments. For charged-particle detection, the acceptance of the detector system depends largely on the energy threshold in the detection and on particle momenta, whereas the acceptance of the π^0 detection system has nonzero values down to zero π^0 momentum. Although the detection of photons ($E_\gamma\approx100$ MeV) requires a large volume of scintillator, we may expect less biased data from the π^0 measurements. The counter measurement of the decay processes of hypernuclei has just started. π^0 detection should be one of the powerful ways of probing the decay processes.

ACKNOWLEDGMENTS

The authors thank professor G. T. Ewan for help in the construction of the experimental setup. We also thank the late Professor H. Bandō, and Professor K. Itonaga and Professor T. Motoba for valuable discussions on the weak decay of hypernuclei. We wish to thank Professor T. Nishikawa, Professor H. Sugawara, Professor H. Hirabayashi, and Professor K. Nakai, and the crew of the KEK 12-GeV proton synchrotron for the support of the experiment. This work was partially supported by the Grant-in-Aid for Special Project Research on Meson Science of the Japan Ministry of Education, Science and Culture, and was partially supported by the Bundesministerium für Forschung und Technologie.

*Present address: Department of Physics, Hiroshima University, Hiroshima 730, Japan.

†Present address: Department of Physics, University of Tokyo, Tokyo 113, Japan.

[1] R. H. Dalitz, Phys. Rev. **112**, 605 (1958); R. H. Dalitz and L. Liu, Phys. Rev. **116**, 1312 (1959).

[2] H. Bandō and H. Takaki, Phys. Lett. **150B**, 409 (1985).

[3] T. Motoba, K. Itonaga, and H. Bandō, Nucl. Phys. **A489**, 683

(1988).

[4]M. A. Faessler, G. Heinzelmann, K. Kilian, U. Lynen, H. Piekarz, J. Piekarz, B. Pietrzyk, B. Povh, H. G. Ritter, B. Schürlein, H. W. Siebert, V. Soergel, A. Wagner, and A. H. Walenta, Phys. Lett. **46B**, 468 (1973).

[5]W. Brückner, M. A. Faessler, K. Kilian, U. Lynen, B. Pietrzyk, B. Povh, H. G. Ritter, B. Schürlein, H. Schröder, and A. H. Walenta, Phys. Lett. **55B**, 107 (1975); W. Brückner, B. Granz, D. Ingham, K. Kilian, U. Lynen, J. Niewisch, B. Pietrzyk, B. Povh, H. G. Ritter, and H. Schröder, Phys. Lett. **62B**, 481 (1976).

[6]R. Grace, P. D. Barnes, R. A. Eisenstein, G. B. Franklin, C. Maher, R. Rieder, J. Seydoux, J. Szymanski, W. Wharton, S. Bart, R. E. Chrien, P. Pile, Y. Xu, R. Hackenburg, E. Hungerford, B. Bassalleck, M. Barlett, E. C. Milner, and R. L. Stearns, Phys. Rev. Lett. **55**, 1055 (1985); P. D. Barnes and J. J. Szymanski, in Proceedings of the 1986 INS International Symposium on Hypernuclear Physics (unpublished), p. 136.

[7]Preliminary report of this work was presented in Proceedings of the 1988 International Symposium on Hypernuclear and Low-Energy Kaon Physics [A. Sakaguchi *et al.*, Nuovo Cimento A **102**, 511 (1989)], and in Proceedings of the 23th Yamada Conference on Nuclear Weak Process and Nuclear Structure, Osaka, Japan, 1989 (unpublished), p. 479.

[8]The first direct measurement of a π^0 particle from the mesonic decay of the $^{4}_{\Lambda}$He hypernucleus was reported by R. Levi Setti and W. E. Slater in Phys. Rev. **111**, 1395 (1958). They observed a $^{4}_{\Lambda}\mathrm{He}\rightarrow{}^{4}\mathrm{He}+\pi^0$, $\pi^0\rightarrow\gamma+e^+ +e^-$ decay. The first investigation of the π^0 decay branching ratio was reported by M. M. Block *et al.* in Proceedings of the International Conference on Hypernuclei, 1964, CERN Report No. 64-1 (unpublished), p. 63. They assumed no decay prong events in the helium bubble chamber as the π^0 decay events of the $^{4}_{\Lambda}$He hypernucleus.

[9]T. Yamazaki, T. Ishikawa, K. H. Tanaka, Y. Akiba, M. Iwasaki, S. Ohtake, H. Tamura, M. Nakajima, T. Yamanaka, I. Arai, T. Suzuki, F. Naito, and R. S. Hayano, Phys. Rev. Lett. **54**, 102 (1985).

[10]S. Kurokawa, H. Hirabayashi, and E. Kikutani, Nucl. Instrum. Methods **212**, 91 (1983).

[11]R. H. Dalitz, D. H. Davis, and D. N. Tovee, Nucl. Phys. **A450**, 311c (1986).

[12]A. Montwill, P. Moriarty, D. H. Davis, T. Pniewski, T. Sobczak, O. Adamovic, U. Krecker, G. Coremans-Bertrand, and J. Sacton, Nucl. Phys. **A234**, 413 (1974).